

Recognition of Smac-mimetic compounds by the BIR domain of cIAP1

Federica Cossu,¹ Francesca Malvezzi,¹ Giulia Canevari,¹ Eloise Mastrangelo,^{1,2} Daniele Lecis,³ Domenico Delia,³ Pierfausto Seneci,^{4,5} Carlo Scolastico,^{4,5} Martino Bolognesi,¹ and Mario Milani^{1,2*}

¹Dipartimento di Scienze Biomolecolari e Biotecnologie, Università di Milano, Via Celoria 26, I-20133, Milano, Italy

²CNR Consiglio Nazionale delle Ricerche-Istituto di Biofisica, Via Celoria 26, I-20133, Milano, Italy

³Dipartimento di Oncologia Sperimentale-Fondazione IRCCS Istituto Nazionale dei Tumori, Via Amadeo 42, I-20133, Milano, Italy

⁴Centro Interdisciplinare Studi bio-molecolari e applicazioni Industriali (CISI), Università di Milano, Via Venezian 21, I-20133, Milano, Italy

⁵Dipartimento di Chimica Organica e Industriale, Università di Milano, Via Venezian 21, I-20133, Milano, Italy

Received 22 July 2010; Revised 27 September 2010; Accepted 28 September 2010

DOI: 10.1002/pro.523

Published online 15 October 2010 proteinscience.org

Abstract: Inhibitor of apoptosis proteins (IAPs) are negative regulators of apoptosis. As IAPs are overexpressed in many tumors, where they confer chemoresistance, small molecules inactivating IAPs have been proposed as anticancer agents. Accordingly, a number of IAP-binding pro-apoptotic compounds that mimic the sequence corresponding to the N-terminal tetrapeptide of Smac/DIABLO, the natural endogenous IAPs inhibitor, have been developed. Here, we report the crystal structures of the BIR3 domain of cIAP1 in complex with Smac037, a Smac-mimetic known to bind potently to the XIAP-BIR3 domain and to induce degradation of cIAP1, and in complex with the novel Smac-mimetic compound Smac066. Thermal stability and fluorescence polarization assays show the stabilizing effect and the high affinity of both Smac037 and Smac066 for cIAP1- and cIAP2-BIR3 domains.

Keywords: apoptosis; IAP family; Smac-mimetics; oncology; cIAP1; BIR3 domain

Introduction

The cellular process of apoptosis is essential for homeostasis maintenance in multicellular organisms,¹ being controlled by a subset of caspases (Cysteine-dependent ASPartyl-specific proteASES) that are regulated, among others, by members of the IAP (Inhibitor of Apoptosis Proteins) family.^{2,3} Specific members of the IAP family, XIAP (X-chromosome-linked IAP), cIAP1 and cIAP2 (cellular IAPs), have

been extensively investigated in the last few years and proposed as drug targets, as they are known to be abnormally expressed at high levels in the majority of human malignancies.⁴ IAPs are composed of one to three tandem BIR (Baculoviral IAP Repeat) domains (BIR1-3) and of a C-terminal RING domain endowed with E3 ubiquitin ligase activity. It has been extensively reported that XIAP and cIAPs act differently: cIAP1 and cIAP2 participate in TNF α -induced NF- κ B activation,⁵ whereas XIAP inhibits apoptosis binding to the initiator caspase-9⁶ and to caspase-3 and -7 (executioner caspases), mainly via its BIR3 and linker-BIR2 domains.^{7,8} IAPs are endogenously antagonized by Smac/DIABLO (Second Mitochondria-derived Activator of Caspases/Direct IAP Binding with LOw pI)^{9,10} through the interaction of the N-terminal AVPI tetrapeptide of the latter with the BIR3 domains of IAPs. It has been recently shown that synthetic compounds based on the Smac

Abbreviations: BIR, baculoviral IAP repeat; cIAPs, cellular IAPs; IAPs, inhibitor of apoptosis proteins; IBM, IAP binding motif; Smac/DIABLO, second mitochondria-derived activator of caspases/direct IAP binding with LOw pI; XIAP, X-linked IAP.

Grant sponsor: Fondazione Cariplo; Grant number: #2009-2534.

*Correspondence to: Mario Milani, Department of Biomolecular Sciences and Biotechnology, University of Milano, Via Celoria 26, 20133-Milano, Italy. E-mail: mario.milani@mi.infm.it

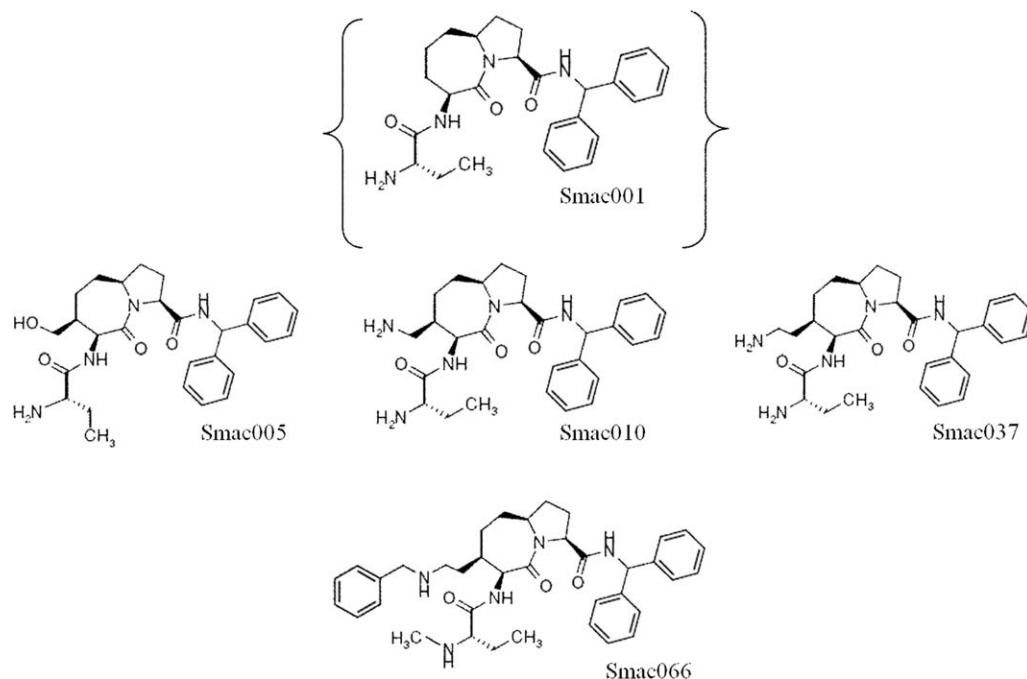


Figure 1. Chemical structures of Smac005, Smac010, Smac037, and Smac066. Note the four different substitutions in the fourth position of the central ring. In brackets the chemical structure of Smac001.¹³

N-terminal AVPI sequence^{11–16} can bind to the BIR domains of IAPs, relieving caspase binding through a competitive mechanism, thus promoting apoptosis.^{17–20} In addition, recent results have shown that Smac-mimetic compounds can kill cancer cells by inducing the “ubiquitin-dependent” degradation of cIAP1 and cIAP2.^{18,19,21}

Starting from a synthetic compound proposed by Sun *et al.*¹³ (Smac001, Fig. 1: 20-fold more potent than the natural Smac AVPI peptide in binding the XIAP-BIR3 domain), we generated a library of 4-substituted azabicyclo[5.3.0]alkane compounds displaying high BIR3 binding affinities.¹⁶ In the last 2 years, Mastrangelo *et al.*¹⁴ and Cossu *et al.*¹⁵ carried over two studies based on X-ray crystallographic, simulative and functional data on the protein/ligand complexes formed by the BIR3 domain of XIAP and three different Smac-mimetics (Smac005, Smac010, and Smac037) displaying different 4-substitutions ($-\text{CH}_2-\text{OH}$, $-\text{CH}_2-\text{NH}_3^+$, and $-\text{CH}_2-\text{CH}_2-\text{NH}_3^+$, respectively, see Fig. 1). These studies showed that, in relation to the different substituents, Smac037 displayed the highest affinity for XIAP-BIR3 and induced cIAP1 degradation in the MDA-MB231 cell line.

However, compared to other derivatives, Smac037 did not show optimal membrane permeability in *in vitro* profiling ADMET tests.¹⁴ To enhance Smac037 lipophilicity, gain beneficial effects on cytotoxicity, and promote its intracellular uptake, Seneci *et al.* designed Smac066,¹⁶ where a methyl group has been added to the terminal amine and the 4-substituent in the central ring has been further elongated to produce a more apolar arm (resulting in $-\text{CH}_2-\text{CH}_2-\text{NH}-\text{CH}_2-\text{Phe}$

nyl, Fig. 1). Smac066 presents low nanomolar potency on XIAP-linkerBIR2BIR3 and on the MDA-MB231 cell line, but also low micromolar potency on HL-60 and PC-3 cells.¹⁶ This compound may thus represent an early lead to be further characterized and optimized *in vitro* and *in vivo*. Moreover, as several examples of bivalent Smac-mimetics that simultaneously bind to different BIRs of the same IAP molecule¹² have been reported as very potent pro-apoptotic agents (i.e., SM164),^{22,23} we also considered Smac066 4-substituent as a Smac-mimetics dimerization platform. In particular, the addition of a $-\text{CH}_2-\text{Phenyl}$ group, resembling the linker portion that joins the two SM164 mimic heads, allowed us to study a potential linker to produce bivalent molecules, in terms of rigidity patterns, possible binding ability, spacing characteristics, and bioavailability.

Here, we characterize the binding affinity of four known Smac-mimetics (Smac001, 005, 010, and 037) together with Smac066 to the cIAP1- and cIAP2-BIR3 domains through fluorescence polarization assays.²² Next, using thermal stability assays on both cIAP1-BIR3 and cIAP2-BIR3 domains, we explore the stabilization induced in both protein domains following the addition of Smac001, Smac005, Smac010, Smac037, and Smac066. Furthermore, we present the crystal structures of cIAP1-BIR3 in complex with Smac037 and with Smac066, highlighting details of the Smac-mimetics binding modes and validating hypotheses put forward by our previous molecular modelling/docking study.¹⁵ Analysis of the crystal structures is presented at the light of the known binding mode of the AVPI tetrapeptide to the IBM

Table I. Fluorescence Polarization Assay. *In Vitro* EC₅₀ Values and Standard Errors for the Different Smac-mimetics in Complex with cIAP1- (left) and cIAP2-BIR3 (right), Measured over Three Independent Experiments

	cIAP1-BIR3			cIAP2-BIR3		
	Log EC ₅₀	EC ₅₀	SE%	Log EC ₅₀	EC ₅₀	SE%
Smac001	0.4	2.6	21.1	0.6	3.7	8.6
Smac005	0.6	3.6	25.6	0.8	6.2	6.9
Smac010	0.3	1.9	17.6	0.6	3.9	7.2
Smac037	0.04	1.1	25.8	0.5	3.6	7.3
Smac066		NA			NA	

(IAP Binding Motif) groove of cIAP1-BIR3 reported by Kulathila *et al.*²⁴ and of the ligand binding mode observed for the XIAP-BIR3/Smac037 complex.¹⁵

Considering the structural conservation of the IBM groove in the BIR3 domains of cIAPs, and at the light of our thermal stability assays on cIAP2-BIR3, we finally tested *in vitro* the capabilities of Smac037 and Smac066 to induce cIAP1 and cIAP2 degradation in the MDA-MB231 cell line, as previously shown for cIAP1 after treatment with Smac005, 010, and 037.¹⁵

Results

Fluorescence polarization assays

Binding and displacement assays based on fluorescent polarization were used to evaluate the affinities

of the synthesized Smac-mimetics for the cIAP1- and cIAP2-BIR3 domains. EC₅₀ values are reported in Table I.

We first performed two saturation binding experiments to determine the binding affinity of the fluorescent probe (Smac-5F) to cIAP1- and cIAP2-BIR3 domain. Under our experimental conditions, the K_d values were evaluated as 4.8 ± 0.6 nM for cIAP1-BIR3 and 23.6 ± 1.6 nM for cIAP2-BIR3 (Fig. 2, panel A), in agreement with the previous results by Lu *et al.*²² Competitive binding assays revealed that all compounds tested displayed low nanomolar EC₅₀ values: Smac037 and Smac001 showed the greatest affinity for cIAP1-BIR3 and cIAP2-BIR3, compared to the other compounds of this series. The EC₅₀ value for Smac066 could not be obtained,

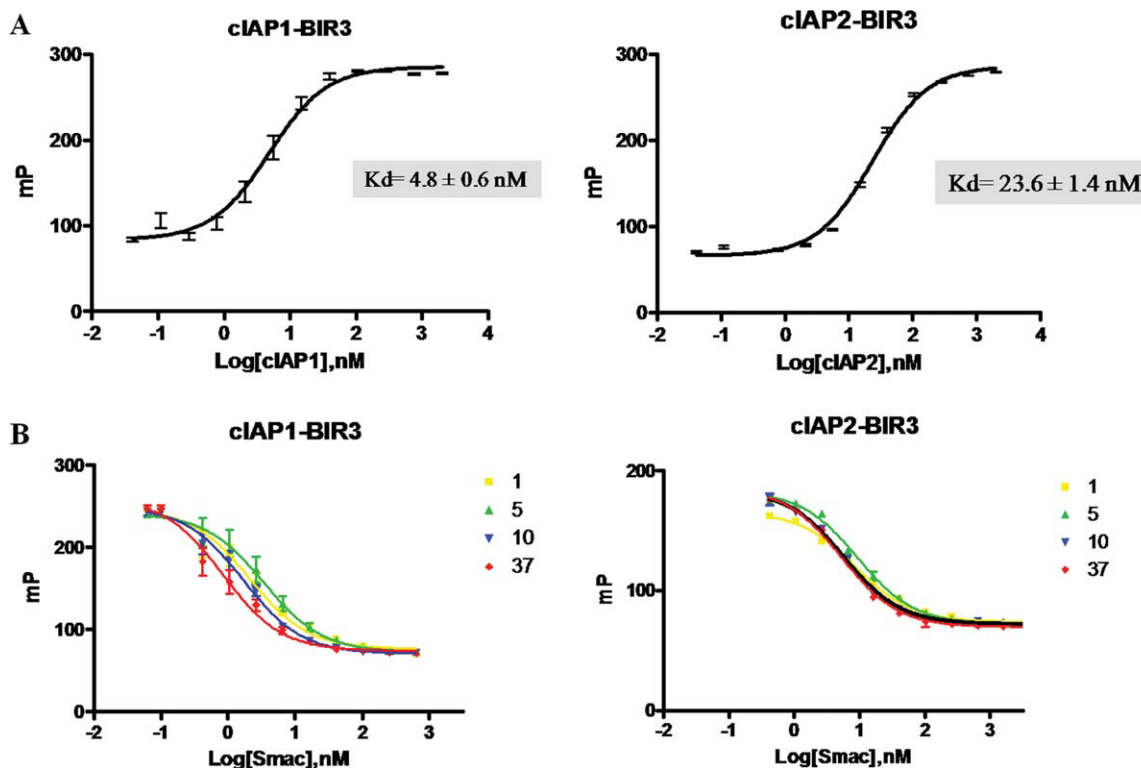


Figure 2. Fluorescence Polarization Assays. (A) Fluorescence polarization saturation curves of the probe used (2 nM) mixed with increasing concentrations of recombinant cIAP1- (left) and cIAP2-BIR3 (right). (B) Displacement of the fluorescent probe from cIAP1- (left) and cIAP2-BIR3 (right) using the unsubstituted Smac001 as matched up-control and the three 4-substituted azabicyclo[5.3.0]alkane Smac-mimetics (Smac005, Smac010, and Smac037). The symbols represent Smac001 (■), Smac005 (▲), Smac010 (▼), and Smac037 (◆). The curve for Smac066 is not reported because its affinity exceeds the sensitivity limit of the probe.

Table II. Melting Temperatures ($^{\circ}\text{C}$) of the cIAP1-BIR3 and cIAP2-BIR3 Domains Alone and Relative Increase in the T_m in Presence of the Selected Smac-mimetics, Reported as the Difference (ΔT_m) Between the Adducts and the Proteins Alone. The T_m Are Determined by Three Independent Experiments

	cIAP1-BIR3	cIAP2-BIR3
Water	58.7 ± 0.3	49.1 ± 0.8
Smac001	+27.1	+23.6
Smac005	+28.0	+25.2
Smac010	+24.5	+21.8
Smac037	+25.8	+21.9
Smac066	+24.6	+21.1

because its affinity is too high relative to that of the fluorescent probe.

Melting temperature shift assays

Thermal shift assay is an experimental technique monitoring fluorescence variations reported by a protein-bound dye during protein thermal denaturation. We take the ΔT_m values as indicative of the amount of stabilization induced by the ligands tested. The T_m values measured for the cIAP1- and cIAP2-BIR3 constructs showed shifts of about 20°C toward higher temperatures when the proteins were bound to reference Smac mimetics (Smac001, 005, and 010), which bear different substituent groups in the fourth position of the central ring,¹⁴ and to Smac037 and Smac066, which host a longer 4-substituted azabicyclo[5.3.0]alkane arm ($-\text{CH}_2-\text{CH}_2-\text{NH}_3^+$ and $-\text{CH}_2-\text{CH}_2-\text{NH}-\text{CH}_2-\text{Phenyl}$, respectively, as reported in Fig. 1). The presence of an elongated amino substituent in Smac037 yielded a more pronounced stabilizing effect on the XIAP-BIR3 domain relative to other reference Smac mimetic compounds.¹⁴ On the contrary, Smac037 higher stabilization was not observed for the BIR3 domain of cIAPs.

In detail, the cIAP1-BIR3 and the cIAP2-BIR3 isolated domains displayed a T_m of $58.7 \pm 0.3^{\circ}\text{C}$ and $49.1 \pm 0.8^{\circ}\text{C}$, respectively. Smac010 binding resulted in the minimum stabilization, with average ΔT_m values of $+24.5$ and $+21.8^{\circ}\text{C}$ when tested on cIAP1- and cIAP2-BIR3, respectively. Smac005 displayed the highest T_m values among the compounds tested (average ΔT_m values on three independent measurements of $+28.0^{\circ}\text{C}$ for cIAP1-BIR3 and $+25.2^{\circ}\text{C}$ for cIAP2-BIR3). Although the effects on T_m are clear cut, suggesting that among the compounds tested on the cIAP1- and cIAP2-BIR3 domains, Smac037 and Smac066 do not represent the most stabilizing ligands (ΔT_m shifts of $+25.8^{\circ}\text{C}$ and $+24.6^{\circ}\text{C}$ for cIAP1-BIR3/Smac037 and /Smac066, respectively, and $+21.9^{\circ}\text{C}$ and $+20.8^{\circ}\text{C}$ for cIAP2-BIR3/Smac037 and /Smac066, respectively), such assays must be taken only as a qualitative indication of their affinities for the different BIR domain constructs. Nevertheless, the T_m data suggest that the positively

charged 4-substituent (as in Smac010 and Smac037) is less effective than the $-\text{CH}_2\text{OH}$ substituent (of Smac005) in defining the Smac-mimetic affinity for cIAP1- and cIAP2-BIR3 domains, whereas the Smac066 4-substituent does not result in a significant stabilization effect when compared to the other Smac-mimetics tested (Table II).

cIAP1-BIR3/Smac037 and /Smac066 complex structures

Analysis of the binding modes of Smac037 and Smac066 to cIAP1-BIR3 were addressed by X-ray crystallography based on crystals of the purified domain grown in the presence of the two Smac-mimetics. The 3D structures were solved through the molecular replacement method using as model the structure of cIAP1-BIR3 reported by Kulathila *et al.*²⁴ in complex with Smac-AVPI; the structures were refined at 2.6 \AA and 3.0 \AA resolution for cIAP1-BIR3/Smac037 and /Smac066, respectively (R_{gen} and R_{free} values together with refinement statistics are reported in Table III). Both crystals display four molecules in the asymmetric unit. Each BIR3 domain is composed of six α -helices (α 1–2 at the N-terminus, and α 3–6 at the C-terminus) and a three-stranded β -sheet; the structure is stabilized by a Zinc-finger motif, conserved in the homologous XIAP-BIR3 domain (Fig. 3, panels A and B). The four independent BIR3 domains display very similar structures, showing r.m.s.d. values in the 0.22 – 0.54 \AA (/Smac037) and 0.41 – 0.62 \AA (/Smac066) ranges (calculated over 110 C α pairs), with significant structural deviations localized at their N- and C-terminal ends only.

After molecular replacement, all BIR3 chains showed strong residual electron density in the IBM groove, comprised between the β 3 strand and the α 3 helix, roughly lined by residues Gly306, Arg308, Cys309, Glu311, Asp314, Glu319, and Trp323. Such residual electron density could be modelled and refined as bound Smac037 and Smac066 moieties (Fig. 3, panels A and B). Also, about 11 amino acids in the C-terminal α helix, not present in the initial model of cIAP1-BIR3/Smac037 structure, were built during the refinement. When compared to the structure of Smac037 in complex with cIAP1-BIR3, the structure of cIAP1-BIR3 in presence of Smac066 presents higher B values (average B values of the BIR3 domain/ligands of $24.1/19.6 \text{ \AA}^2$ for the first structure vs. $64.4/72.3 \text{ \AA}^2$ for the second structure). Finally, chain D from cIAP1-BIR3/Smac066 structure displays high level of mobility in the crystal, showing elevated B -factor values over the whole chain (average B value of 53.7 \AA^2 over chains A, B and C; 106.6 \AA^2 over chain D).

It should be noticed that, in both crystal structures, crystal packing does not result in direct intermolecular contacts to any of the Smac-mimetic

Table III. X-ray Data-Collection and Refinement Statistics for the cIAP1-BIR3/Smac037 and /Smac066 Complexes

	cIAP1-BIR3/Smac037	cIAP1-BIR3/Smac066
Data Collection Statistics		
Space group	C2	C222
Unit-cell parameters (Å)	$a = 71.6 \text{ \AA}, b = 79.8 \text{ \AA}, c = 98.4 \text{ \AA},$ $\alpha = \gamma = 90^\circ, \beta = 92.5^\circ$	$a = 113.6 \text{ \AA}, b = 114.6 \text{ \AA},$ $c = 92.9 \text{ \AA}, \alpha = \gamma = \beta = 90^\circ$
Solvent content %	50.8	51.2
<i>N</i> of molecules per a.u.	4	4
Resolution (Å)	98.3 - 2.6	92.9 - 3.0
Mosaicity (°)	1.3	0.8
No of unique reflections	15,911 (2,377)	11,909 (1,745)
Completeness (%)	93.3 (96.3)	96.3 (98.0)
Redundancy	2.3 (2.3)	3.8 (3.9)
Rmerge ^a (%)	9.3 (36.9)	12.7 (59.2)
Average <i>I</i> / σ (<i>I</i>)	5.5 (2.0)	7.4 (2.0)
Refinement statistics		
R factor ^b (%)	22.6	19.2
<i>R</i> _{free} ^c (%)	28.8 ^d	25.7 ^e
r.m.s. Bond lengths (Å)	0.009	0.010
r.m.s. Bond angles (°)	1.06	1.12
Average protein <i>B</i> factor (Å ²)	24.2	66.9
Ramachandran Plot		
Residues in most favoured regions (%)	86,0%	89,0%
Residues in additionally allowed regions (%)	13,4%	9,8%

Values in parentheses are for the highest resolution shell.

^a $R_{\text{merge}} = \sum |I - \langle I \rangle| / \sum I \times 100$, where *I* is intensity of a reflection and $\langle I \rangle$ is its average intensity.

^b $R_{\text{factor}} = \sum |F_o - F_c| / \sum |F_o| \times 100$.

^c *R*_{free} is calculated on 5% randomly selected reflections, for cross-validation.

^d 798 reflections

^e 575 reflections.

compounds, thus not affecting the binding mode of the Smac-mimetics to the cIAP1-BIR3 IBM pocket.

The cIAP1-BIR3/Smac-mimetics binding modes

As mentioned above, in all four chains of the crystal asymmetric unit, the ligand molecules are bound to the IBM groove, exchanging hydrogen bonds with main chain of residues Gly306, Arg308, and Cys309 ($\beta 3$ strand) and salt bridges with the side chains of residues Glu311, Asp314, Glu319 (in $\beta 3$ - $\alpha 3$ loop and in $\alpha 3$).

Trp323 is one of the most conserved residues within the IBM grooves of known IAP BIR3 domains. Its side chain has been shown to establish van der Waals interactions with the pyrrolidine ring of a conserved Pro in the IBMs of Smac/DIABLO and Caspase-9, and with the corresponding central ring moiety of the Smac-mimetic molecules reported so far in our^{14,15,25} and other available structures of IAP complexes.^{26,27} Such interaction occurs also in the complex structures here presented (Fig. 3, C and D), where the side chain of cIAP1-BIR3 Trp323 stacks on the seven-carbon central ring of Smac037 and Smac066 (distances of $4.0 \pm 0.5 \text{ \AA}$). A second stacking interaction (π -cation interaction) is provided by Arg308, whose guanidine group is parallel to/and localizes at $3.9 \pm 0.3 \text{ \AA}$ from the Smac037 and Smac066 phenyl moiety adjacent to the cIAP1-BIR3 $\beta 3$ strand (Fig. 3, panels C and D). Details of

all interactions stabilizing the cIAP1-BIR3/Smac037 and /Smac066 complexes are listed in Table IV and displayed in Fig. 3, panels C and D.

The cIAP1-BIR3/Smac-mimetics structures shed light on the role played by the 4-substituent groups ($-\text{CH}_2\text{CH}_2\text{NH}_3^+$ and $-\text{CH}_2\text{CH}_2\text{NHCH}_2\text{Phenyl}$) relative to complex stabilization. Inspection of the cIAP1-BIR3/Smac037 crystal structure suggests that the 4-substituent affects the Smac-mimetic location due to a negative surface patch (Glu311, Asp314, Glu319) that attracts the two charged amino groups in the 4-substituent arm and in the N-terminal portion of Smac037. Such “pulling effect” is likely responsible for repositioning Smac037 in the IBM pocket relative to the XIAP-BIR3/Smac037 complex,¹⁵ and may be one of the factors defining the lower melting temperatures measured for the cIAP1-BIR3/Smac010 and /Smac037 complexes (both bearing an amino 4-substituent) compared to cIAP1-BIR3/Smac001 and /Smac005 (Table II). In fact, small shifts of Smac010 and Smac037 within the IBM groove may result in weaker β -like interactions with the BIR3 domain $\beta 3$ strand, as discussed below.

Although the long 4-substituent on Smac066 appears disordered in the solvent, we observed the same shift in the Smac-mimetic position within the BIR3 active pocket as in Smac037. In fact, at the crystallization pH both Smac066 *N*-methyl and the secondary amine in the 4-substituent “arm” are

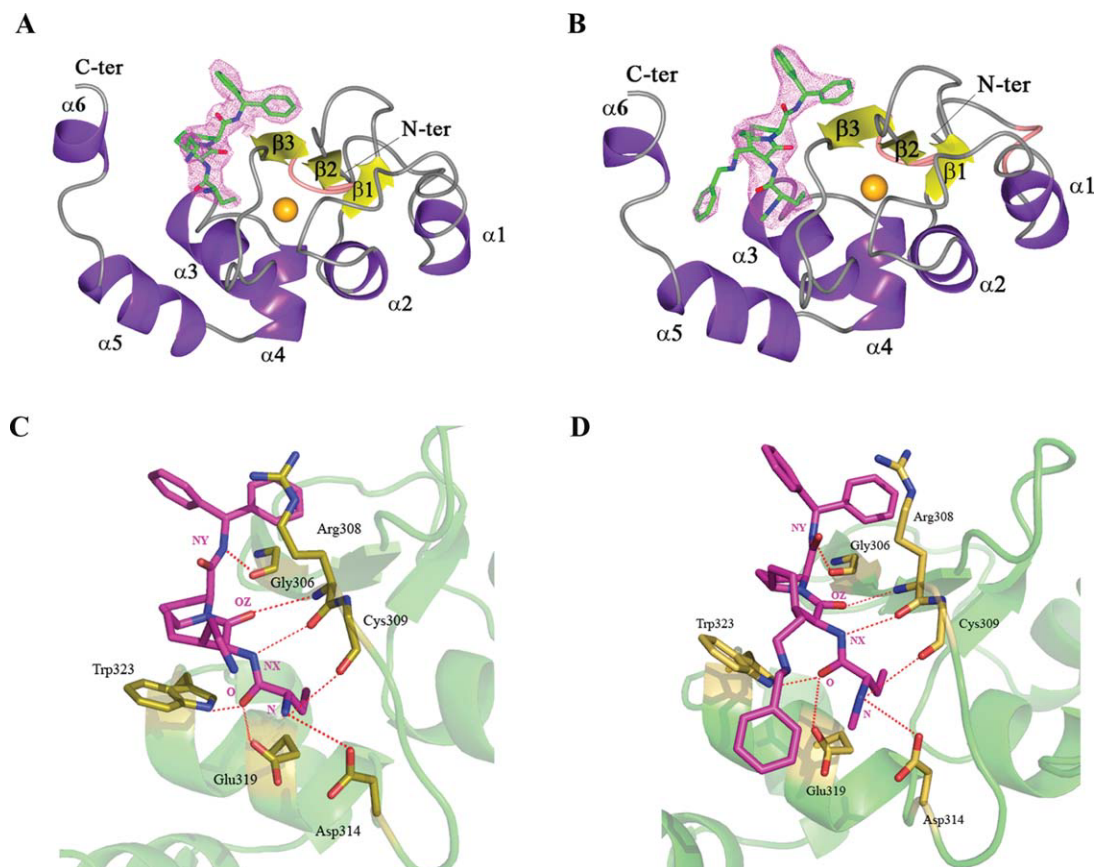


Figure 3. Overall architecture of cIAP1-BIR3/Smac037 and /Smac066 complexes (A, B) and details of the cIAP1-BIR3 interaction with Smac037 and Smac066 (C, D). (A, B) The cIAP1-BIR3 molecule is drawn according to its secondary structure: the six α -helices building BIR3 are shown in purple, the three anti-parallel β -strands in yellow, the two β -turns in pink, and, finally, coiled regions are represented in grey. The core Zn-atom is represented as an orange sphere. The magenta cage shows the Fo-Fc difference Fourier map (contoured at 7.5σ), calculated after few refinement cycles of the protein structure alone. The difference electron density falls in the IBM groove, comprised between the $\beta 3$ strand and the $\alpha 3$ helix, where the Smac-mimetics bind (panel A, Smac037; panel B, Smac066) (represented in fat bonds coloured by atom with green carbons, blue nitrogens, and red oxygens). (C, D) The main residues involved in stabilizing interactions with the Smac-mimetics are labelled and shown in gold. The Smac-mimetics are represented in fat bonds with magenta carbons, nitrogen atoms in blue, and oxygens in red; the Smac-mimetics interacting atoms are labelled in magenta; cIAP1-BIR3 overall structure is shown in light green. The main hydrogen bonds linking BIR3 and the Smac-mimetics are shown as red dashed lines (drawn with PyMOL⁴¹).

positively charged and thus subjected to the pooling effect of the protein negative patch. Such observation is in agreement with the similar thermal shift values observed for Smac37 and Smac66 ($\Delta T_m = +25.8$ and $+24.6$, respectively). Fluorescence polarization assays, however, show that Smac066 affinity for cIAP1- and 2-BIR3 domains remains very high, effectively exceeding the sensitivity limit of the FP technique. Such an effect could be due to a role played by the hydrophobic moiety on the Smac66 4-substituent arm that is not evident in our structural analysis.

Relative positioning of Smac037 and AVPI in the IBM groove of cIAP1

Inspection of the cIAP1-BIR3/Smac037 crystal structure here reported compared to that of the cIAP1-BIR3/Smac-AVPI complex (PDB code 3D9U)²⁴ shows

a r.m.s. displacement of $0.38\text{--}0.48 \text{ \AA}$ (over 92 C α pairs); according to expectations, the protein/peptide mimetic and the protein/peptide interactions are closely similar in the two complexes (Fig. 4, panel A). Specific interactions gained or lost in the cIAP1-BIR3/Smac037 binding mode, when compared to the BIR3/AVPI complex are summarized in Table IV. In general, there is an overall shift of Smac037 relative to AVPI toward the negative patch, mentioned above (about 0.5 \AA), but also away from the $\beta 3$ strand (about 0.8 \AA). These shifts are probably due to a concerted effect of a “pulling action” on the positive charges of Smac037 by the negative patch of the IBM groove, and of a “pushing effect” provided by Trp310 toward the Smac037 N-terminal ethyl moiety. In fact, such ethyl substituent of Smac037 is bulkier than the Ala side chain in AVPI, potentially resulting in a collision with the side chain of Trp310

Table IV. Hydrogen Bonds Distances in Å Measured for cIAP1-BIR3/Smac037 in Comparison with cIAP1BIR3/Smac066 (A), cIAP1-BIR3/AVPI (B), and XIAP-BIR3/Smac037 (C). Distances for the Complex Structures Here Reported Have Been Measured as an Average of the Four Independent Observations in the Asymmetric Unit

(A) cIAP1-BIR3/Smac037 in Comparison with cIAP1BIR3/Smac066						
037/066	Gly306 {O}	Arg308 {O} {N}	Cys309 {O}	Asp314 {Oδ2}	Glu319 {Oε1}	Trp323 {Nε1}
NY	2.8 ± 0.1/3.0 ± 0.2					
NX		3.2 ± 0.1/3.0 ± 0.4				
OZ		3.2 ± 0.1/2.9 ± 0.3				
N			3.2 ± 0.1/ 3.6 ± 0.5	3.3 ± 0.1/ 3.4 ± 0.7		
O					3.3 ± 0.2/ 3.9 ± 0.3	3.8 ± 0.2/ 3.9 ± 0.3
(B) cIAP1-BIR3/Smac037 in Comparison with cIAP1-BIR3/AVPI						
037/AVPI	Gly306 {O}	Arg308 {O} {N}	Cys309 {O}	Asp314 {Oδ2}	Glu319 {Oε1}	Trp323 {Nε1}
NY/Ile4 {N}	2.8 ± 0.1/2.9					
NX/Val2 {N}		3.2 ± 0.1/2.9				
OZ/Val2{O}		3.2 ± 0.1/ 2.8				
N/Ala1{N}			3.2 ± 0.1	3.3 ± 0.1/2.8	2.9	
O/Ala1{O}					3.3 ± 0.2/3.5	3.8 ± 0.2/3.1
(C) cIAP1-BIR3/Smac037 in Comparison with XIAP-BIR3/Smac037						
cIAP1/XIAP	Gly306 {O}	Arg308 {O}*/{N} Thr308 {O}*/{N}	Cys309 {O} Asp309 {O}	Asp314 {Oδ2} Glu314 {Oδ1/2}	Glu319 {Oε1} Gln319 {Oε1}	Trp323 {Nε1}
037/NY	2.8 ± 0.1/3.3					
037/NX		3.2 ± 0.1*/2.9*				
037/OZ		3.2 ± 0.1/3.2				
037/N			3.2 ± 0.1/ 3.2	3.3 ± 0.1/2.9/3.0		
037/O					3.3 ± 0.2/3.8	3.8 ± 0.2/3.3

that would require a 0.8 Å displacement to be released.

Relative positioning of Smac037 in the IBM groove of cIAP1 and XIAP

The binding mode of Smac037 to cIAP1-BIR3 is also similar to that observed for the same ligand on XIAP-BIR3 (Fig. 4, panel B). In fact, the XIAP-BIR3 residues involved in van der Waals contacts (Val298, Lys299, and Trp310) and hydrogen bonds (Gly306, Leu307, and Trp323) with the inhibitory compounds are conserved, except for Leu292, replaced by Val in cIAPs; XIAP Glu314 is conservatively substituted with Asp in cIAP1, while Gln319 is Glu319 in cIAP1 (and Gln319 in cIAP2). Finally, residues Thr308 and Asp309 that were found relevant for the interaction of XIAP-BIR3 with the Smac-mimetics are replaced in cIAPs by Arg308 and Cys309 (Fig. 4, panel C). As expected, the hydrogen bonds that involve the cIAP1- and XIAP-BIR3 β3 backbone are generally maintained, with significant variations concerning the residues belonging to the β3-α3 loop. First, the presence of Asp314 in cIAP1 (Glu314 in XIAP) causes the sliding of Smac037 toward such residue (and toward the cIAP1 negative patch Glu311, Asp314, and Glu319, which in XIAP hosts Lys311, Glu314 and Gln319, respectively) to establish optimal electrostatic interactions (Fig. 4, panel B). Besides, the nonconservative substitution of XIAP-

BIR3 Lys311 with Glu311 in cIAP1-BIR3 makes the negative pocket more attractive compared to the XIAP-BIR3 homologous patch, where the Smac-mimetic shift is not observed.

In conclusion, although the Smac037 interaction network is generally conserved among the two BIR3 domains, there are some amino acid substitutions that, on the whole, slightly weaken Smac037 binding to cIAP1-BIR3 relative to XIAP-BIR3, shifting the ligand of about 1.5 Å toward the negative patch described.

cIAPs degradation by Smac-mimetics in MDA-MB231 cell line

Although apoptotic regulation is performed differently by XIAP and cellular IAPs, these members of the IAP family are structurally homologous. XIAP shows an amino acid sequence identity to cIAP1 and cIAP2 of 36% and 39%, respectively, whereas the amino acid sequence identity between cIAP1 and cIAP2 is 70%. In particular, the region of BIR3 domain, where are located the critical residues involved in Smac-mimetics recognition, is well conserved among the three IAPs analyzed (Fig. 4, panel C). As a consequence of such prominent structural conservation, Smac-mimetics are shown to be broadly effective on the most characterized members of the IAP family: they mimic Smac/DIABLO in preventing XIAP inhibition of initiator and effector

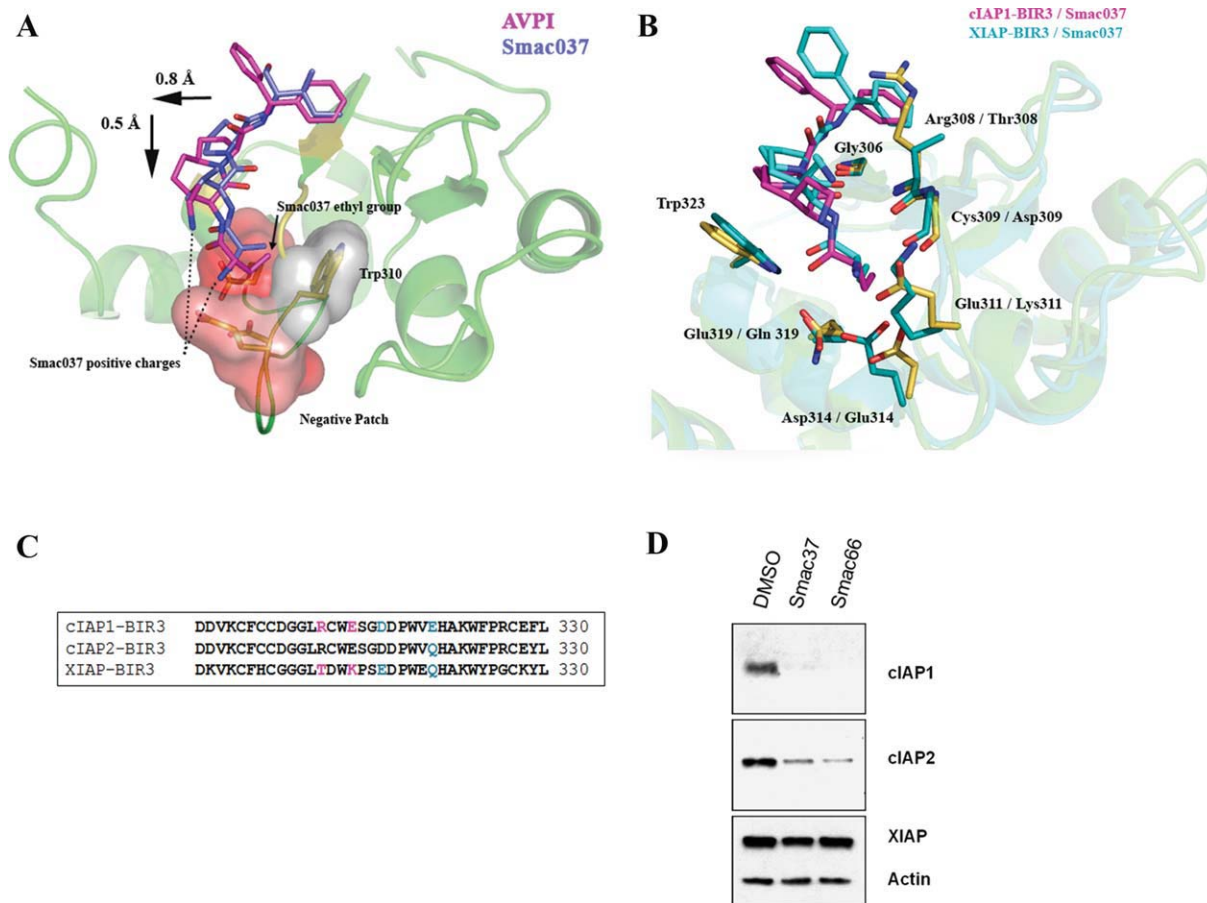


Figure 4. cIAP1-BIR3/SmacAVPI and cIAP1-BIR3/Smac037 superposition (A), XIAP-BIR3/Smac037 and cIAP1-BIR3/Smac037 structure superposition (B), cIAP1-BIR3, cIAP2-BIR3, and XIAP-BIR3 alignment (C), and cIAP2 degradation assay (D). (A) The superposition of cIAP1-BIR3/SmacAVPI and cIAP1-BIR3/Smac037 highlights the relative locations of Smac AVPI (light blue) and Smac037 (magenta) once bound to cIAP1-BIR3 (green ribbons). The interacting residues in cIAP1-BIR3 are represented in gold. The figure also reports the detail of the negative patch composed by the negatively charged residues Glu311, Asp314 and Glu319, that produces a Smac037 displacement of 0.5 Å relative to Smac AVPI towards the negative patch. The hydrophobic region designed by Trp310 side chain is also shown in grey, to evidence its role in the Smac037 shift of 0.8 Å relative to Smac AVPI, away from the β3 strand (structure and surfaces drawn with Pymol⁴¹). (B) XIAP-BIR3/Smac037 and cIAP1-BIR3/Smac037 superposition: cIAP1-BIR3 (green ribbons, 60% transparency) binding groove residues are in gold sticks, corresponding XIAP-BIR3 (cyan ribbons, 60% transparency) residues are highlighted in cyan. Substituted residues are labeled as follows (cIAP-BIR3/XIAP-BIR3). Smac037 in complex with cIAP1-BIR3 is reported in magenta, whereas the ligand in complex with XIAP-BIR3 is shown in cyan sticks. (C) The cIAP1-BIR3 and XIAP-BIR3 IBM-specific groove sequence alignment: the nonconservatively substituted residues are reported in magenta, whereas the residues that are conservatively substituted are reported in light blue. (D) cIAPs degradation in presence of Smac037 and Smac066 in MDA-MB231 cell line. The blot was normalized for the levels of b-Actin. The DMSO lane refers to untreated cells.

caspases, and in parallel they can kill malignant cells by inducing auto-degradation of cIAP1 and cIAP2, thus leading to TNF-receptor mediated apoptosis.^{18,19,21}

The melting temperature shifts of cIAP1- and cIAP2-BIR3 induced by the Smac-mimetic compounds here considered and the crystal structures provide evidence of efficient Smac-mimetic binding to the target proteins, that result in XIAP seizure and cIAPs auto-ubiquitination. Based on the high amino acid sequence conservation of the three IAP family members, in particular between cIAP1-BIR3 and cIAP2-BIR3 (Fig. 4, panel C), we speculated that the Smac-mimetics here discussed could also

bind to the cIAP2-BIR3 domain. For this reason, we tested *in vitro* the effects of Smac037 and of Smac066 in inducing both cIAPs degradation in the MDA-MB-231 cell line, as previously reported for the cIAP1-BIR3 domain after cell treatment with Smac005, 010, and 037.¹⁵ The Western blot analysis showed that Smac037 and 066 effectively induce the degradation of cIAP1¹⁵ but not completely that of cIAP2 (Fig. 4, panel D). In fact, it has been shown that abrogation of Smac-mimetics-induced apoptosis can occur by upregulation of cIAP2, which although initially degraded, is refractory to subsequent degradation.²⁸ This suggests that cIAP2 may require the presence of cIAP1 for its own ubiquitination, like

other IAPs²⁹; on the other hand, cIAP1 degradation induced by Smac-mimetics may prevent the complete removal of cIAP2, whose upregulation may result in the long-term restoration of cellular IAPs activity. These results, together with the structural details of the cIAP1-BIR3/Smac037 and cIAP1-BIR3/Smac066 complexes, provide new hints for the development of lead compounds able to bind XIAP, cIAP1, and cIAP2, thus acting in different apoptotic pathways.

Discussion

IAPs are crucial players in the major apoptotic pathways, and their blockade seems to be one of the most promising strategies for tumor suppression. The identification of lead compounds mimicking the natural antagonist of IAPs, Smac/DIABLO, is now the focus of extensive research, as it has been broadly reported that Smac-mimetics induce apoptosis in many neoplastic cell lines, especially in combination with other chemotherapies, as recently reported by Lecis *et al.*³⁰ for melanoma cell line. The Smac-mimetics proposed in this study present high affinity for cIAP1- and 2-BIR3 in fluorescence binding assays and high stabilization ability on the protein construct tested, suggesting enhanced capability to specifically recognize the active pockets on the target IAP proteins. The crystal structures here described provide new ideas for the design of more potent drug leads, which can be accurately developed for the BIR3 domains of XIAP and cIAP1. In particular, the small number of amino acid differences in IAPs BIR3 highlight three regions in the Smac-mimetic compounds that can be exploited to modulate affinity for the diverse proteins. (1) Smac-mimetic phenyl end: the π -cation interaction with Arg308 in cIAPs is not present in XIAP (substituted by Thr309), and the hydrophobic cavity hosting the phenyl moiety is smaller in cIAPs (lined by Val292) than in XIAP (Leu292). (2) Smac-mimetic 4-substituent arm: it is possible to modulate its interaction with amino acid 309 (Cys in cIAPs and Asp in XIAP). (3) Smac-mimetic N-terminal end interacts with the IBM negative patch that is wider and more charged in cIAPs than in XIAP. As a general consequence, referring to points 1 and 3, we can speculate that a limited extension of a Smac-mimetic compound both at its phenyl and N-terminal ends could maintain its affinity for cIAPs-BIR3, reducing that for XIAP.

In addition, as bivalent Smac-mimetic molecules have been reported as very potent agents on tumors,²² mobile noninteractive portions of the Smac-mimetics could be elongated to allow the design of bivalent compounds, simultaneously targeting different BIR domains of the same IAP. In this context, the addition of Smac066 4-substituent¹⁶ could be a useful tool to begin the characterization

of different linkers joining two Smac-mimetic heads. In particular, a noninteractive linker would be preferable, to favor the Smac-mimetic/IBM groove interactions only and avoid secondary binding motives that would produce an impairment of the usual IAPs-Smac-mimetics recognition. In the cIAP1-BIR3/Smac066 structure here reported, the Smac066 4-substitution meets such requirement, being free in the solvent and exposed enough to be linked to a second Smac-mimetic molecule. Although the crystal packing here observed may not be consistent with the real distances between the BIR of the same IAP molecule, and with their relative positions, the structure here described provides general ideas on how to join two Smac-mimetic heads, to be subsequently tested in a wider drug design study.

All the efforts in Smac-mimetics optimization rely on the fact that they are versatile compounds, acting on different IAP members that are involved in distinct apoptotic pathways; these small molecules competitively bind to the IBM pocket of XIAP, preventing caspase inhibition, and induce cIAPs degradation, as shown here. Although the former activity has been extensively described, the molecular mechanism by which Smac-mimetics produce cIAPs auto-ubiquitination has not been defined yet. In this context, further structural and functional characterization of the full length cIAP proteins may be of prime interest.

Materials and Methods

Chemistry

All the Smac-mimetics were synthesized following the procedures described.^{14,15} The chemical procedure for Smac066 synthesis and the rational bases for its design are reported by Seneci *et al.*,¹⁶ where Smac066 is named as “40d.” Smac037 and Smac066 were suspended in water at a final concentration of 0.1M.

Cloning, expression, and purification of human cIAP1-BIR3

The sequence coding for cIAP1- and cIAP2-BIR3 domains residues 245-357 (XIAP-BIR3 structural homology numbering) were cloned in pET21(a) vector (Novagen) with a C-terminal 6xHis-tag. The plasmids were used to transform *Escherichia coli* strain BL21(DE3). The recombinant proteins were purified using Ni-NTA (His-trap FFcrude, Ge-Healthcare), followed by gel filtration (Superdex 200, Ge-Healthcare). The recombinant proteins were eluted in 20 mM Tris pH 8.0, 250 mM NaCl, and 10 mM DTT, and cIAP1-BIR3 was concentrated to 10 mg mL⁻¹ for crystallization tests using an Amicon Ultra centrifugal filter (10 kDa cut-off).

Fluorescence polarization assays

Fluorescence polarization experiments were performed according to Lu *et al.*²² Briefly, the fluorescently labelled Smac peptide SM5F (AbuRPF-K(5-Fam)-NH₂, final concentration of 2 nM), and increasing concentrations of cIAP1- and cIAP2-BIR3 from 0 to 20 μM, were added to an assay buffer consisting of 100 mM potassium phosphate, pH 7.5, 100 μg/mL bovine γ-globulin, 0.02% sodium azide. After shaking (15 min), the plate was incubated for 3 h at room temperature. Fluorescence polarization was measured on an Ultra plate reader (Tecan), at excitation and emission wavelengths of 485 nm and 530 nm, respectively. The equilibrium binding curves were drawn by plotting experimental data (millipolarization units, mP) as a function of recombinant concentration. All experiments were performed in black, flat-bottom 96-well microplates (Greiner bio-one).

Four-substituted azabicyclo[5.3.0]alkane Smac-mimetics were evaluated for their ability to displace the fluorescent probe from recombinant protein. Fluorescent probe (2 nM), cIAP1-BIR3 (10 nM) or cIAP2 (25 nM) and serial dilutions of 4-substituted azabicyclo[5.3.0]alkane Smac-mimetics (concentration ranging from 4 μM to 0.4 nM) were added to each well, to a final volume of 125 μL in the assay buffer described above. After 15 min mixing on a shaker, and 3 h incubation at room temperature, fluorescent polarization was measured on the Ultra plate reader (Tecan). The EC₅₀ values are shown in Table I.

Melting temperature shift assays

To monitor protein unfolding, the fluorescent dye Sypro Orange, an environmentally sensitive dye, was used. The fluorescence intensity increases during protein unfolding because the fluorescent dye binds efficiently to the unfolded protein, and displays a higher quantum yield in a lower dielectric environment. The melting temperatures are calculated as the maximum in the first derivative of the recorded sigmoid. The overall continuous decrease of the fluorescence intensity, after unfolding, is due to dye decay and, likely, to aggregation of the denatured protein–dye complexes.³¹

Thermal shift assays for the different Smac-mimetics were conducted in a MiniOpticon Real-Time PCR Detection System (Bio-Rad). Solutions of 2.2 μL of the cIAP1 or cIAP2 BIR protein were mixed with 3.5 μL of Sypro orange (Sigma) diluted 1:60, 19 μL of the respective buffers, and 0.3 μL of 50 mM Smac-mimetics (Smac001, Smac005, Smac010, Smac037, and Smac066). Distilled water was added in place of the inhibitors for the control samples. The final protein concentrations ranged between 0.4 and 0.5 mg/mL; the sample plates were heated from 4 to 99°C, with a heating rate of 0.2°C/5 sec. Fluorescence intensity was measured within the

excitation/emission ranges 470–505/540–700 nm. All the experiments were performed in triplicate to produce an average T_m value and an error estimation (Table II).

Crystallization and crystallographic data reduction

Sitting drop crystallization experiments were prepared using an Oryx-8 crystallization robot (Douglas Instruments, East Garston, UK), from a 2:1 mixture of the protein stock solution (provided with 5 mM of Smac037 and of Smac066) and the precipitant solution to a final drop volume of 0.3 μL for the initial screenings and of 0.5 μL for the optimization trials. After 4 days of vapour diffusion at 20°C, one irregular globular crystal of cIAP1-BIR3 in complex with Smac037 of ~80 μm³ was obtained in 25% PEG 3350, 0.1M Hepes pH 7.5 and 0.2M Lithium Sulphate. A prismatic crystal for the complex cIAP1-BIR3/Smac066 was obtained after 4 days of vapor diffusion at 20°C in 25% PEG 3350, 0.1M Tris, pH 8.0, and 0.1M Sodium Citrate. Before being fresh-cooled in liquid nitrogen, the crystal for the cIAP1-BIR3/Smac037 was soaked in paraffin, whereas the crystal of the complex with Smac066 was harvested in a cryoprotectant solution (25% PEG 400, 0.1M Tris, pH 8.0, 0.1M Sodium Citrate and 25% glycerol). The crystals diffracted to a maximum resolution of 2.6 Å for the complex with Smac037 and of 3.0 Å for Smac066, using synchrotron radiation on beam-line ID 14-4, at the European Synchrotron Radiation Facility (ESRF-Grenoble, France). The diffraction data were processed with MOSFLM,³² and intensities were merged using SCALA.³³

Structure determination and refinement

The cIAP1-BIR3/Smac037 and /Smac066 crystals belong to the C2 and C222 space groups with unit cell parameters $a = 71.4$, $b = 79.7$, $c = 98.3$ Å (Smac037 complex) and $a = 113.6$, $b = 114.6$, $c = 92.9$ Å (Smac066 complex); in both cases, there are four protein molecules in the crystal asymmetric unit ($V_M = 2.5$ Å³ Da⁻¹, 51% solvent content for both complexes).³⁴ The crystal structure was solved with molecular replacement (molrep³⁵), using the structure of the BIR3 domain in the cIAP1-BIR3/SmacAVPI complex (PDB code 3D9U²⁴) as search model. The four independent molecules were subjected to rigid-body refinement ($R/R_{free} = 42.0/41.3$ for the cIAP1-BIR3/Smac037 complex, $R/R_{free} = 42.2/44.6$ for the cIAP1-BIR3/Smac066), and subsequently refined using REFMAC5.³⁶ A random set comprising 5% of the data was omitted from refinement for R-free calculation. Manual rebuilding³⁷ and additional refinement³⁸ were subsequently performed. Inspection of difference Fourier maps at this stage showed strong residual density, located between the α3 helix and the main β-sheet, compatible with one Smac-mimetic inhibitor

for each molecule in the asymmetric unit, which was accordingly model-built. The last refinement cycles have been performed using program Buster³⁸ with TLS (Translation Libration Screw-motion) and NCS (Non crystallographic symmetry) restraints.

The refined cIAP-BIR3/Smac037 and /Smac066 models display almost the entire amino acid chain; the first 12 N-terminal residues (241–253) and the last 2 C-terminal residues are disordered. Data collection and refinement statistics are summarized in Table I. The stereochemical quality of the models was checked using the program Procheck³⁹ and is summarized in the Table I. Atomic coordinates and structure factors for cIAP1-BIR3/Smac037 and /Smac066 complexes have been deposited with the Protein Data Bank⁴⁰ with accession codes **3MUP** and **3OZ1**, respectively.

IAP degradation cell-based assays

The MDA-MB231 cell line was treated with 5 μ M of Smac037 or Smac066, or left untreated as control. After 3 h, cells were harvested and lysed. Proteins were revealed by Western blot using antibodies specific for XIAP (BD Biosciences), cIAP1 and cIAP2 (R&DSYSTEMS), and β Actin (Sigma) as control.

References

1. Steller H (1995) Mechanisms and genes of cellular suicide. *Science* 267:1445–1449.
2. Deveraux QL, Reed JC (1999) IAP family proteins—suppressors of apoptosis. *Genes Dev* 13:239–252.
3. LaCasse EC, Baird S, Korneluk RG, MacKenzie AE (1998) The inhibitors of apoptosis (IAPs) and their emerging role in cancer. *Oncogene* 17:3247–3259.
4. Vischioni B, van der Valk P, Span SW, Kruyt FA, Rodriguez JA, Giaccone G (2006) Expression and localization of inhibitor of apoptosis proteins in normal human tissues. *Hum Pathol* 37:78–86.
5. Rothe M, Pan MG, Henzel WJ, Ayres TM, Goeddel DV (1995) The TNFR2-TRAF signaling complex contains two novel proteins related to baculoviral inhibitor of apoptosis proteins. *Cell* 83:1243–1252.
6. Shiozaki EN, Chai J, Rigotti DJ, Riedl SJ, Li P, Srinivasula SM, Alnemri ES, Fairman R, Shi Y (2003) Mechanism of XIAP-mediated inhibition of caspase-9. *Mol Cell* 11:519–527.
7. Riedl SJ, Renatus M, Schwarzenbacher R, Zhou Q, Sun C, Fesik SW, Liddington RC, Salvesen GS (2001) Structural basis for the inhibition of caspase-3 by XIAP. *Cell* 104:791–800.
8. Wang CY, Mayo MW, Korneluk RG, Goeddel DV, Baldwin AS, Jr (1998) NF-kappaB antiapoptosis: induction of TRAF1 and TRAF2 and c-IAP1 and c-IAP2 to suppress caspase-8 activation. *Science* 281:1680–1683.
9. Du C, Fang M, Li Y, Li L, Wang X (2000) Smac, a mitochondrial protein that promotes cytochrome c-dependent caspase activation by eliminating IAP inhibition. *Cell* 102:33–42.
10. Verhagen AM, Ekert PG, Pakusch M, Silke J, Connolly LM, Reid GE, Moritz RL, Simpson RJ, Vaux DL (2000) Identification of DIABLO, a mammalian protein that promotes apoptosis by binding to and antagonizing IAP proteins. *Cell* 102:43–53.
11. Nikolovska-Coleska Z, Wang R, Fang X, Pan H, Tomita Y, Li P, Roller PP, Krajewski K, Saito NG, Stuckey JA, Wang S (2004) Development and optimization of a binding assay for the XIAP BIR3 domain using fluorescence polarization. *Anal Biochem* 332:261–273.
12. Li L, Thomas RM, Suzuki H, De Brabander JK, Wang X, Harran PG (2004) A small molecule Smac mimic potentiates TRAIL- and TNFalpha-mediated cell death. *Science* 305:1471–1474.
13. Sun H, Nikolovska-Coleska Z, Yang CY, Xu L, Liu M, Tomita Y, Pan H, Yoshioka Y, Krajewski K, Roller PP, Wang S (2004) Structure-based design of potent, conformationally constrained Smac mimetics. *J Am Chem Soc* 126:16686–16687.
14. Mastrangelo E, Cossu F, Milani M, Sorrentino G, Lecis D, Delia D, Manzoni L, Drago C, Seneci P, Scolastico C, Rizzo V, Bolognesi M (2008) Targeting the X-linked inhibitor of apoptosis protein through 4-substituted azabicyclo[5.3.0]alkane smac mimetics. Structure, activity, and recognition principles. *J Mol Biol* 384:673–689.
15. Cossu F, Mastrangelo E, Milani M, Sorrentino G, Lecis D, Delia D, Manzoni L, Seneci P, Scolastico C, Bolognesi M (2009) Designing Smac-mimetics as antagonists of XIAP, cIAP1, and cIAP2. *Biochem Biophys Res Commun* 378:162–167.
16. Seneci P, Bianchi A, Battaglia C, Belvisi L, Bolognesi M, Caprini A, Cossu F, Franco E, Matteo M, Delia D, Drago C, Khaled A, Lecis D, Manzoni L, Marizzoni M, Mastrangelo E, Milani M, Motto I, Moroni E, Potenza D, Rizzo V, Servida F, Turlizzi E, Varrone M, Vasile F, Scolastico C (2009) Rational design, synthesis and characterization of potent, non-peptidic Smac mimics/XIAP inhibitors as proapoptotic agents for cancer therapy. *Bioorg Med Chem* 17:5834–5856.
17. Oost TK, Sun C, Armstrong RC, Al-Assaad AS, Betz SF, Deckwerth TL, Ding H, Elmore SW, Meadows RP, Olejniczak ET, Oleksijew A, Oltersdorf T, Rosenberg SH, Shoemaker AR, Tomaselli KJ, Zou H, Fesik SW (2004) Discovery of potent antagonists of the antiapoptotic protein XIAP for the treatment of cancer. *J Med Chem* 47:4417–4426.
18. Vince JE, Wong WW, Khan N, Feltham R, Chau D, Ahmed AU, Benetatos CA, Chunduru SK, Condon SM, McKinlay M, Brink R, Leverkus M, Tergaonkar V, Schneider P, Callus BA, Koentgen F, Vaux DL, Silke J (2007) IAP antagonists target cIAP1 to induce TNFalpha-dependent apoptosis. *Cell* 131:682–693.
19. Varfolomeev E, Blankenship JW, Wayson SM, Fedorova AV, Kayagaki N, Garg P, Zobel K, Dynek JN, Elliott LO, Wallweber HJ, Flygare JA, Fairbrother WJ, Deshayes K, Dixit VM, Vucic D (2007) IAP antagonists induce autoubiquitination of c-IAPs, NF-kappaB activation, and TNFalpha-dependent apoptosis. *Cell* 131:669–681.
20. Zobel K, Wang L, Varfolomeev E, Franklin MC, Elliott LO, Wallweber HJ, Okawa DC, Flygare JA, Vucic D, Fairbrother WJ, Deshayes K (2006) Design, synthesis, and biological activity of a potent Smac mimetic that sensitizes cancer cells to apoptosis by antagonizing IAPs. *ACS Chem Biol* 1:525–533.
21. Petersen SL, Wang L, Yalcin-Chin A, Li L, Peyton M, Minna J, Harran P, Wang X (2007) Autocrine TNFalpha signaling renders human cancer cells susceptible to Smac-mimetic-induced apoptosis. *Cancer Cell* 12:445–456.
22. Lu J, Bai L, Sun H, Nikolovska-Coleska Z, McEachern D, Qiu S, Miller RS, Yi H, Shangary S, Sun Y, Meagher JL, Stuckey JA, Wang S (2008) SM-164: a novel, bivalent Smac mimetic that induces apoptosis and tumor

- regression by concurrent removal of the blockade of cIAP-1/2 and XIAP. *Cancer Res* 68:9384–9393.
23. Nikolovska-Coleska Z, Meagher JL, Jiang S, Kawamoto SA, Gao W, Yi H, Qin D, Roller PP, Stuckey JA, Wang S (2008) Design and characterization of bivalent Smac-based peptides as antagonists of XIAP and development and validation of a fluorescence polarization assay for XIAP containing both BIR2 and BIR3 domains. *Anal Biochem* 374:87–98.
 24. Kulathila R, Vash B, Sage D, Cornell-Kennon S, Wright K, Koehn J, Stams T, Clark K, Price A (2009) The structure of the BIR3 domain of cIAP1 in complex with the N-terminal peptides of SMAC and caspase-9. *Acta Cryst D* 65:58–66.
 25. Cossu F, Milani M, Mastrangelo E, Vachette P, Servida F, Lecis D, Canevari G, Delia D, Drago C, Rizzo V, Manzoni L, Seneci P, Scolastico C, Bolognesi M (2009) Structural basis for bivalent Smac-mimetics recognition in the IAP protein family. *J Mol Biol* 392:630–644.
 26. Cohen F, Koehler MF, Bergeron P, Elliott LO, Flygare JA, Franklin MC, Gazzard L, Keteltas SF, Lau K, Ly CQ, Tsui V, Fairbrother WJ (2010) Antagonists of inhibitor of apoptosis proteins based on thiazole amide isosteres. *Bioorg Med Chem Lett* 20:2229–2233.
 27. Sun H, Stuckey JA, Nikolovska-Coleska Z, Qin D, Meagher JL, Qiu S, Lu J, Yang CY, Saito NG, Wang S (2008) Structure-based design, synthesis, evaluation, and crystallographic studies of conformationally constrained Smac mimetics as inhibitors of the X-linked inhibitor of apoptosis protein (XIAP). *J Med Chem* 51:7169–7180.
 28. Petersen SL, Peyton M, Minna JD, Wang X (2010) Overcoming cancer cell resistance to Smac mimetic induced apoptosis by modulating cIAP-2 expression. *Proc Natl Acad Sci USA* 107:11936–11941.
 29. Cheung HH, Plenchette S, Kern CJ, Mahoney DJ, Korneluk RG (2008) The RING domain of cIAP1 mediates the degradation of RING-bearing inhibitor of apoptosis proteins by distinct pathways. *Mol Biol Cell* 19:2729–2740.
 30. Lecis D, Drago C, Manzoni L, Seneci P, Scolastico C, Mastrangelo E, Bolognesi M, Anichini A, Kashkar H, Walczak H, Delia D (2010) Novel SMAC-mimetics synergistically stimulate melanoma cell death in combination with TRAIL and Bortezomib. *Br J Cancer* 102:1707–1716.
 31. Pantoliano MW, Petrella EC, Kwasnoski JD, Lobanov VS, Myslik J, Graf E, Carver T, Asel E, Springer BA, Lane P, Salemme FR (2001) High-density miniaturized thermal shift assays as a general strategy for drug discovery. *J Biomol Screen* 6:429–440.
 32. Steller I, Bolotovskiy R, Rossmann MG (1997) An algorithm for automatic indexing of oscillation images using Fourier analysis. *J Appl Cryst* 30:1036–1040.
 33. Collaborative Computational Project N (1994) The CCP4 Suite: programs for protein crystallography. *Acta Cryst D* 50:760–763.
 34. Matthews BW (1968) Solvent content of protein crystals. *J Mol Biol* 33:491–497.
 35. Vagin AA, Teplyakov A (1997) MOLREP: an automated program for molecular replacement. *J Appl Cryst* 30:1022–1025.
 36. Winn MD, Isupov MN, Murshudov GN (2001) Use of TLS parameters to model anisotropic displacements in macromolecular refinement. *Acta Cryst D* 57:122–133.
 37. Emsley P, Cowtan K (2004) Coot: model-building tools for molecular graphics. *Acta Cryst D* 60:2126–2132.
 38. Blanc E, Roversi P, Vonrhein C, Flensburg C, Lea SM, Bricogne G (2004) Refinement of severely incomplete structures with maximum likelihood in BUSTER-TNT. *Acta Cryst D* 60:2210–2221.
 39. Laskowski RA, Rullmannn JA, MacArthur MW, Kaptein R, Thornton JM (1996) AQUA and PROCHECK-NMR: programs for checking the quality of protein structures solved by NMR. *J Biomol NMR* 8:477–486.
 40. Berman HM, Westbrook J, Feng Z, Gilliland G, Bhat TN, Weissig H, Shindyalov IN, Bourne PE (2000) The Protein Data Bank. *Nucleic Acids Res* 28:235–242.
 41. DeLano WL (2002) The PyMOL molecular graphic system. San Carlos, CA, USA: DeLano Scientific.